

pubs.acs.org/acschemicalbiology Articles

## Radical-Mediated Covalent Azidylation of Hydrophobic Microdomains in Water-Soluble Proteins

Benjamin B. Minkoff, Heather L. Burch, Jamison D. Wolfer, and Michael R. Sussman\*



Cite This: ACS Chem. Biol. 2023, 18, 1786–1796



**Read Online** 

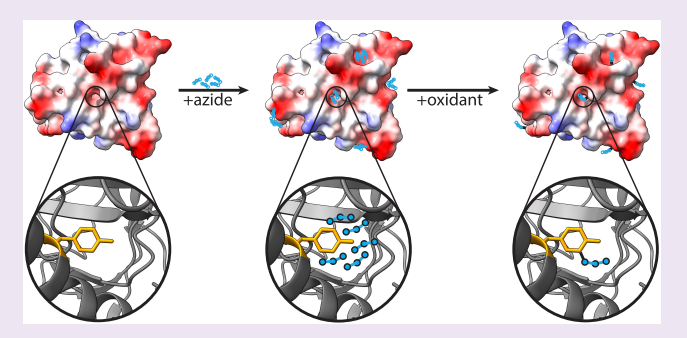
**ACCESS** 

III Metrics & More

Article Recommendations

s Supporting Information

**ABSTRACT:** Hydrophobic microdomains, also known as hydrophobic patches, are essential for many important biological functions of water-soluble proteins. These include ligand or substrate binding, protein—protein interactions, proper folding after translation, and aggregation during denaturation. Unlike transmembrane domains, which are easily recognized from stretches of contiguous hydrophobic sidechains in amino acids via primary protein sequence, these three-dimensional hydrophobic patches cannot be easily predicted. The lack of experimental strategies for directly determining their locations hinders further understanding of their structure and function. Here, we posit that the small triatomic anion  $N_3^-$  (azide) is attracted to these patches



and, in the presence of an oxidant, forms a radical that covalently modifies C-H bonds of nearby amino acids. Using two model proteins (BSA and lysozyme) and a cell-free lysate from the model higher plant *Arabidopsis thaliana*, we find that radical-mediated covalent azidylation occurs within buried catalytic active sites and ligand binding sites and exhibits similar behavior to established hydrophobic probes. The results herein suggest a model in which the azido radical is acting as an "affinity reagent" for nonaqueous three-dimensional protein microenvironments and is consistent with both the nonlocalized electron density of the azide moiety and the known high reactivity of azido radicals widely used in organic chemistry syntheses. We propose that the azido radical is a facile means of identifying hydrophobic microenvironments in soluble proteins and, in addition, provides a simple new method for attaching chemical handles to proteins without the need for genetic manipulation or specialized reagents.

#### 1. INTRODUCTION

Many studies on the folding and unfolding of proteins have indicated that the shielding of short hydrophobic patches from aqueous solution is an important driving force for these dynamic processes. 1,2 To study in-solution protein structure, mass spectrometry-based "footprinting" methods use a wide range of covalent amino acid-modifying reagents, including the water-soluble hydroxyl (\*OH) radical (HRF, for hydroxyl radical footprinting). Unlike traditional methods such as X-ray crystallography, cryo-EM, and NMR, protein footprinting can provide considerable insights without limitations on size, purity, and amount. Footprinting provides critical information on the location of solvent-accessible and solvent-inaccessible amino acid sidechains and corroborates information derived from high-resolution structures when available, as determined by traditional means.

For this purpose, initially within the above context of radical-mediated covalent protein labeling, we considered the azido radical. There are currently three methods to introduce an azide group into a protein, but none involve direct azido radical-mediated processes, as are used in synthetic organic chemistry with small molecules. These methods are: (1) supplementing messenger ribonucleic acid (mRNA) translation with azide-containing residues in permissible cellular

backgrounds,<sup>6,7</sup> (2) using azide-containing reagents that perform site-specific chemical derivatization, such as maleimide chemistry, *N*-hydroxysuccinimide ester chemistry, or N-terminal derivatization using a pyridine compound,<sup>8</sup> and (3) derivatizing of primary amines to azides using diazo transfer.<sup>9,10</sup> Of these, the third method, i.e., diazo transfer without free radicals, is most comparable to the radical-based method described herein, but the diazo transfer is limited in that at a physiological pH, few amines undergo the conversion, the process takes many hours, and requires specialized reagents not readily available.<sup>10</sup> We reasoned that a method that relies upon azido free radical attack and requires only simple, inexpensive, and safe reagents would find use in protein labeling as a prelude to its additional use in understanding basic principles involved in protein structure and function.

Received: April 18, 2023 Accepted: June 30, 2023 Published: July 18, 2023





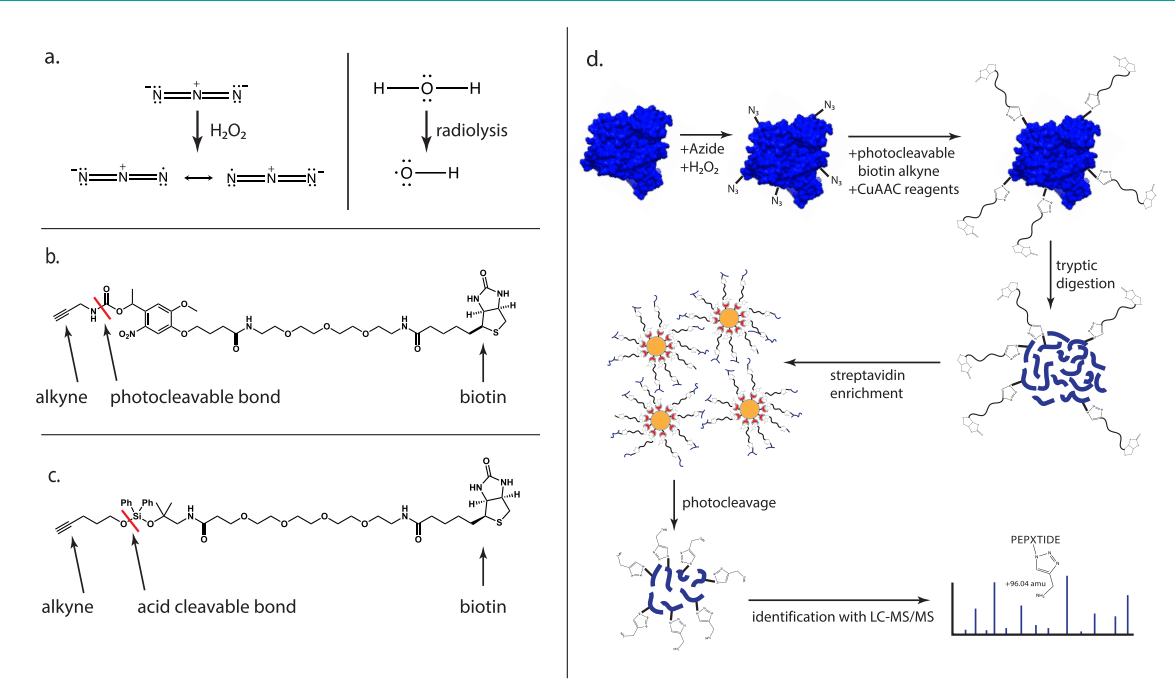


Figure 1. Methodology of oxidative azidylation and detection via mass spectrometry. (a) Although the diatomic hydroxyl radical, created via radiolysis of water, has no delocalized resonance, the triatomic azide free radical delocalizes electron density via resonance. (b, c) Alkynes used in conjunction with copper-catalyzed azide—alkyne cycloaddition (CuAAC) for the detection, enrichment, and mapping of azide covalently bound to protein. (d) Workflow for generation and detection of covalent azidylation, as described in the main text. Note that using the alkyne in (c) results in a +125.06 amu adduct.

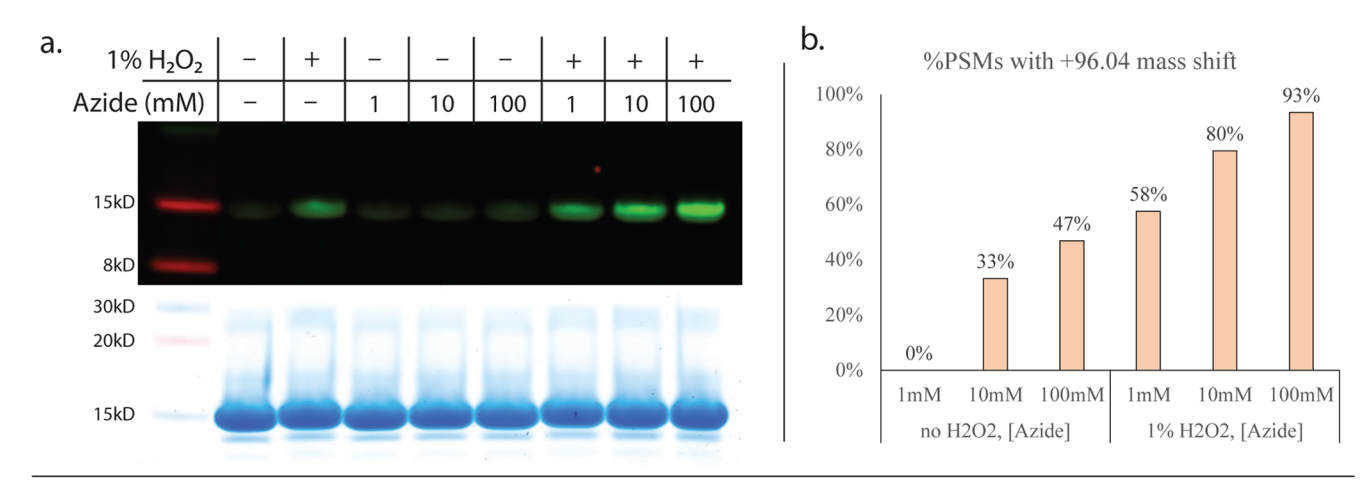
In contrast to the hydroxyl radical, a small, diatomic molecule that lacks delocalized electron density, the azido radical is triatomic and exhibits resonance stabilization via electron density delocalization across the three nitrogen atoms (Figure 1A), providing the capability of short-range pi electron attraction with other aromatic molecules as well as with electron-deficient centers, such as cations. 11 Given this difference between the hydroxyl free radical and the azido radical, we reasoned that developing a method to label protein in solution with azido radicals might complement existing footprinting methods and open new avenues for facile azidebased click derivatization for synthetic protein chemistry.<sup>1</sup> The majority of azide addition chemistry reported in the literature, whether the mechanism involves the azide anion or the neutral azido radical, occurs in organic solvents or in organic/aqueous solvent mixtures and temperatures or pH that are deleterious to proteins maintaining their native, catalytically active three-dimensional folded state. 11,13,14 Because of this, the known body of literature on azidylation chemistry is inapplicable to studying native protein structure. That said, a few reports indicate that azido radicals can covalently modify free amino acids, 15-19 but the majority of data obtained suggest that azido radicals create transient sidechain radicals, which create structures such as dityrosine bridges that lack the azide adduct itself. 20,21 The suggestion that azido radicals can covalently attack aromatic amino acids or ringed olefins 16,17 led us to ask whether azido radicals could directly modify amino acid sidechains in an intact, structured protein context under conditions that are unlikely to denature the three-dimensional structure of proteins, an observation that has not yet been

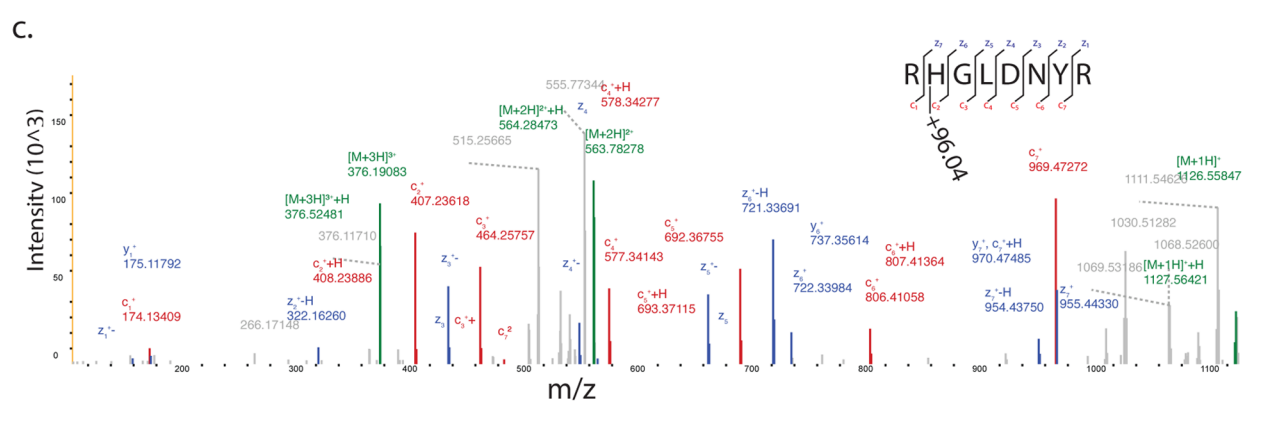
Herein, we report multiple findings related to azide radical-based covalent modification of folded proteins. First, we report that adding sodium azide and  $H_2O_2$  to protein in a

physiological buffer and at neutral pH causes covalent azidylation on multiple residues, which can then be derivatized using the copper-catalyzed azide—alkyne cycloaddition (CuAAC) to add an enrichable handle 12,22 and enables identification of the modified residues via mass spectrometry. Second, our experiments suggest that noncovalent azide:protein binding may be a more widespread phenomenon than previously thought from studies focused on the handful of known metabolic enzymes that it targets noncovalently, such as cytochrome c oxidase and the F1-ATPase. 23 Finally, our cumulative data support a model in which hydrophobicity is a major force driving azide:protein binding.

Thus, it appears azide behaves similarly to the covalent labeling reagent diethylpyrocarbonate (DEPC), which has been reported to modify residues found in transmembrane domains and in soluble proteins, within structured hydrophobic patches. The reactivity of DEPC with soluble proteins is destroyed when the higher-order protein structure is greatly reduced via proteolytic digestion, 4,24-27 and suggests DEPC can empirically identify amino acids present in structured hydrophobic protein microdomains. Underscoring the need for empirical methods to identify hydrophobic microdomains, recent computational studies have indicated that hydrophilic amino acid sidechains are as likely to be present in these hydrophobic microdomains as are the hydrophobic sidechains, confounding the prediction of such patches from the primary sequence.<sup>28</sup> Thus, to further explore this question, it is imperative to utilize orthogonal methods, including reactive reagents such as DEPC and azide to target hydrophobic microdomains.

Overall, we report that the azide anion binds noncovalently to hydrophobic patches only present in structured proteins and can be oxidatively radicalized to create a covalent protein labeling reagent. This azidylation can be derivatized via Click





d. [			# of peptide spectral matches						
				No H2O2		1% H2O2			
Peptide(s)	Residue #s	Site of Modification	1mM Azide	10mM Azide	100mM Azide	1mM Azide	10mM Azide	100mM Azide	
CELAAAMKR	6-14	K13	-	-	-	1	-	40	
RHGLDNYR	14-21	H15	-	-	-	1	-	111	
GYSLGNWVCAAK	22-33	W28	-	-	-	-	25	58	
NTDGSTDYGILQINSR	46-61	Y53	-	-	-	-	-	57	
NLCNIPCSALLSSDITASVNCAK	74-96	188	-	13	31	-	2	52	
IVSDGNGMNAWVAWR	98-112	A110/W111	-	-	-	-	25	63	
GTDVQAWIR	117-125	W123	-	-	-	49	92	118	
		Total PSMs ->	0	13	31	49	144	459	

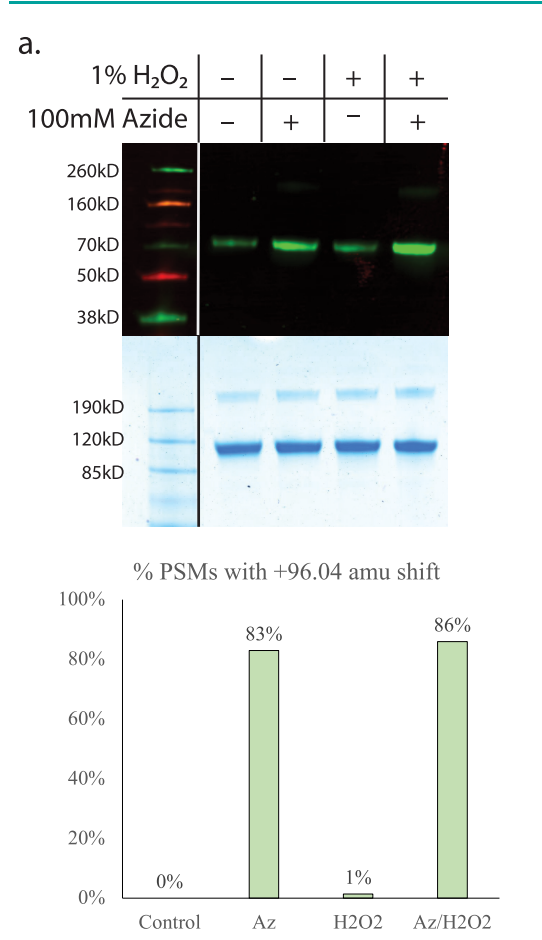
Figure 2. Lysozyme is azidylated in an azide dose-dependent fashion. (a) Both azide and peroxide are necessary for strong, direct lysozyme azidylation. Top: streptavidin blot; Bottom: Coomassie-stained polyacrylamide gel. (b) Increased azidylation is observed when hydrogen peroxide is added to lysozyme and azide. (c) Example MS/MS spectrum showing localization of +96.04 azide adduct on a lysozyme histidine following electron transfer dissociation. Peptide and spectrum are annotated with c- and z-ion series. Due to supplemental collisional fragmentation, y-ions are observed in the spectrum as well. (d) Azidylation increases significantly with increased azide dose in the presence of hydrogen peroxide. Localized sites are denoted in the site of modification column.

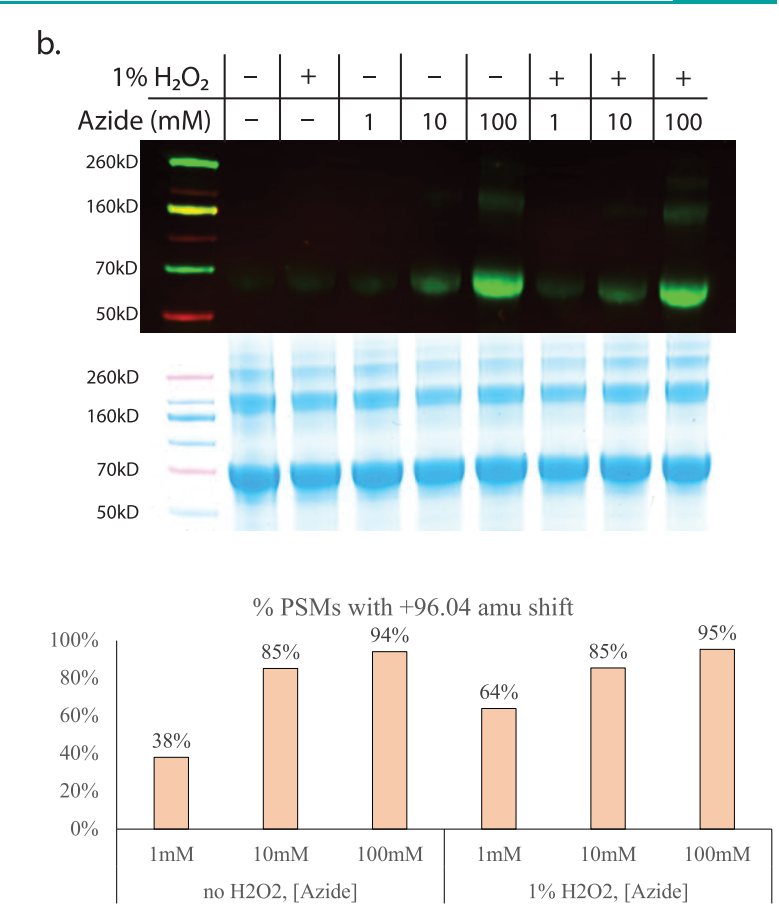
chemistry, captured, and localized using mass spectrometry, the methodology of which lays the foundation for not only an enrichable, covalent handle to map protein hydrophobicity but also a facile, accessible way to activate proteins under physiological conditions for Click derivatization.

#### 2. RESULTS AND DISCUSSION

# **2.1. Method Development and Rationalization.** Classically, azido radicals that interact with free amino acids are generated by linear particle accelerators irradiating water to create hydroxyl radicals, which in turn react with azide to

produce azido radicals. <sup>17,18</sup> Given this, we asked whether more accessible methods of oxidation could facilitate azido radical generation in a physiological buffer system. H<sub>2</sub>O<sub>2</sub> was selected as the oxidant due to its relative ease of use, availability, and reported oxidizing capability in a protein context. <sup>29,30</sup> A publication that reports the addition of azido radicals to free tryptophan suggests that the adduct reaction is inefficient and produces a product with relatively low abundance. <sup>17</sup> Thus, we developed an assay to detect and enrich the modified compound via click chemistry (CuAAC). <sup>31</sup> Using a biotiny-lated and either acid- or photocleavable alkyne allowed the





C.					# PS	SMs		
				no H2O2			1% H2O2	
Peptide(s)	Residues in protein	Site of Modification	1mM Azide	10mM Azide	100mM Azide	1mM Azide	10mM Azide	100mM Azide
FKDLGEEHFK	35-44	H42		40	124		7	115
DLGEEHFK	37-44	П42	-	40	124	<u>-</u>	'	113
TCVADESHAGCEK	76-88	H83	-	-	15	-	-	43
SLHTLFGDELCK	89-100	S89	-	62	170	-	-	170
QEPERNECFLSHKDDSPDLPK	118-138	11120			51		_	124
NECFLSHKDDSPDLPK	123-138	H129	-	-	31	-	-	124
ECCHGDLLECADDRADLAK	267-285	11270	-	-	19	-	-	21
VHKECCHGDLLECADDRADLAK	264-285	H270	-	-	11	-	-	36
SHCIAEVEK	310-318	6210	16	40	197	22	93	380
SHCIAEVEKDAIPENLPPLTADFAEDKDVCK	310-340	S310	16	40	197	22	93	360
DDPHACYSTVFDK	387-399	11200			42		6	96
EYEATLEECCAKDDPHACYSTVFDK	375-399	- H390	-	-	42	-	0	90
LKHLVDEPQNLIK	400-412	H403		6	212		_	253
HLVDEPQNLIK	402-412	п403	-	υ	212	Ī	-	233
LFTFHADICTLPDTEK	529-544	H533	-	-	91	-	-	105

Figure 3. BSA is azidylated in an azide-dependent fashion. (a) Top: Streptavidin blot using a copper and alkyne-based conjugation system visualized by fluorescently-labeled streptavidin. Middle: Coomassie-stained polyacrylamide gel. Ladders and lanes are from separate regions of the same gels and not vertically shifted (gray and black lines, respectively). Bottom: Though fluorescence is observed in lanes without peroxide and azide, no modification is observed via mass spectrometry. (b) BSA azidylation is azide dose-responsive, and at lower concentrations, peroxide causes increased azidylation over azide alone. Top: Streptavidin blot. Middle: Coomassie-stained polyacrylamide gel. Bottom: Similar levels of azidylation are observed via mass spectrometry with 100 mM azide ± peroxide, lower levels with 10 mM azide and added peroxide, and higher levels with 1 mM azide and added peroxide. (c) In BSA, azide dose-dependent azidylation occurs mainly on histidine and serine.

capture of azidylated peptides with streptavidin followed by release using acid or light (Figure 1B,C). These alkynes were chosen because the resulting triazole-linked biotin is detectable with streptavidin blotting and the cleaved mass adduct can be readily detected with tandem mass spectrometry (MS/MS). To map azide adducts, protein is first oxidatively azidylated by

treatment with sodium azide and  $H_2O_2$  at an ambient temperature and a physiological pH, i.e., under conditions unlikely to cause protein unfolding and denaturation. Next, the azidylated protein is derivatized to a triazole linkage using CuAAC and an alkyne, as shown in Figure 1B,C. One can monitor azidylation via either routine sodium dodecyl sulfate—

polyacrylamide gel electrophoresis (SDS-PAGE) and blotting procedures or, as we would strongly recommend, via bottomup mass spectrometry. Briefly, the protein can be separated via SDS-PAGE and blotted with streptavidin to detect clicked-on biotin and, for mass spectrometric-based analysis, protein can be proteolytically digested and the resulting modified peptides enriched with streptavidin and eluted via acid or photocleavage to produce peptides with triazole-containing respective mass adducts of +125.06 or +96.04 amu, whose location within the protein sequence can be determined via high-resolution tandem mass spectrometry (Figure 1D). Finally, we refer the reader to the first methods section detailing azide safety measures. Though the method is relatively easy to perform, and the amounts and volumes of azide used herein are low, azide is a dangerous compound to work with and all precautions should be taken.

2.2. Oxidative Azidylation Modifies Lysozyme. As shown in Figure 2A and Table S1, by adding 1% H2O2 and increasing concentrations of azide to lysozyme for 20 s, increasing azidylation of lysozyme was detected using both blotting and MS. H<sub>2</sub>O<sub>2</sub> addition alone led to a minor increase in blotting, which we attribute to the biotin compound coordinating to a small extent with free lysozyme, and below, bovine serum albumin (BSA). That said, adding azide to the reaction significantly increased the signal, and as shown below, H<sub>2</sub>O<sub>2</sub> alone does not lead to any azidylation observed via MS. High-resolution tandem mass spectrometry was used to confirm the modification mass adduct, to localize azidylation sites and to measure the degree of azidylation (Figure 2B–D). High-energy collisional dissociation (HCD) fragmentation of peptides containing the azide modification revealed that under these conditions, the triazole adduct is partially labile (Figure S1) but could be retained by using electron transfer dissociation with supplemental collisional activation (EThcD), evidenced by both a richer series of fragment ions and the presence of unfragmented precursor (Figures S2-S7). Peptide spectral matches (PSMs) were used here as a semiquantitative means of assaying azidylation level; we found that azidylation events here and with BSA below track as expected across multiple doses of azide using PSMs as a metric

We observed azidylation on multiple residues; modification of histidine, lysine, tryptophan, tyrosine, and isoleucine was confirmed using tandem mass spectra (Figure 2C). Observing lysine and histidine modification suggests that the azide anion may be interacting with positively charged residues; however, mapping the modified residues to the structure revealed that although the charged residues are partially surface exposed, the uncharged ones are buried within an internal cleft sandwiched by helices, which we mechanistically address in detail in Section 2.5 (Figure S8). Surprisingly, we observed azide dosedependent azidylation at residue I88 in the absence of added hydrogen peroxide, which as described in Section 2.3 may be explained by noncovalent azide binding in the first step and oxidation in the second step, i.e., during the subsequent click reaction. This was the only residue that displayed such behavior and adding hydrogen peroxide did not increase its azidylation significantly, which suggests that this event may occur during clicking, detailed below with BSA. All other sites of modification were only identified with added hydrogen peroxide. Samples supplied with 100 mM azide exhibited far more azidylation than those with lower doses.

Green fluorescent protein (GFP) fluorescence, which is proportional to native protein structure, was monitored under identical reaction conditions. From these experiments, we found that no fluorescence was lost, suggesting that the conditions used are not harsh enough to strongly denature GFP. However, letting the reaction continue for 60 s beyond the initial 20 s treatment led to an ~30% loss of fluorescence in azide-containing samples, suggesting that while longer treatments cause unfolding (Figure S9), the conditions utilized here maintain GFP's actively fluorescing structure. Whether or not this extends to proteins with more sensitivity to structural perturbation or that require native chemistry for catalysis will be the subject of future studies.

Though the atomic composition of the azidylation product was first verified with high-resolution mass spectrometry starting with natural abundance 14N-containing azide, commercially available 15N-labeled azide was used as a secondary validation. By following the multiple reaction steps described herein, the final chemical modification should include the heavy isotope-containing azide supplied in the first step. Indeed, when BSA was supplied with <sup>15</sup>N-labeled azide in place of natural abundance 14N azide as described in the following section, we observed mass shifts of +97.04, rather than +96.04 (Figure S10 and Table S2), confirming the supplied azide is present within the final product. Residue level oxidation above control samples or free radical-induced protein crosslinking were not observed (Figures S11 and 2A), suggesting classical sidechain oxidation intermediates, the result of hydroxyl radical modification, are likely not involved in the reaction.

2.3. BSA Binds Azide Noncovalently to Enable "One-Pot" Azidylation and Click Chemistry. To test the azido radical's ability to modify other proteins and further investigate the phenomenon of H<sub>2</sub>O<sub>2</sub>-independent azidylation, another well-studied model protein, bovine serum albumin (BSA), was used. As shown in Figure 3 and Tables S2 and S3, BSA azidylation was detected using both blotting and MS. As seen with lysozyme, there was streptavidin reactivity observed in the absence of either added azide or added H2O2, suggesting that some level of biotin reactivity with free protein is creating a degree of artifactual blotting background. Thus, as with lysozyme, BSA blots as shown in the figures were followed by high-resolution mass spectrometry. H<sub>2</sub>O<sub>2</sub> addition alone did not lead to significant modification (Figure 3A and Table S3) or oxidation above control levels (Figure S11). As observed with lysozyme, the addition of 100 mM azide alone to BSA led to significant azidylation. The effect was clearly azide dosedependent and stronger than with lysozyme (Figure 3B,C)—at 100 mM supplied azide, levels of azidylation were virtually identical regardless of added hydrogen peroxide. At 10 mM azide, slightly less azidylation was observed in the H<sub>2</sub>O<sub>2</sub>containing samples, and at 1 mM azide, significantly less azidylation was observed when H<sub>2</sub>O<sub>2</sub> was not added. Thus, the phenomenon observed with lysozyme was also observed with BSA—at lower azide levels, H<sub>2</sub>O<sub>2</sub> is necessary for BSA azidylation, whereas at higher azide concentrations, detectable azidylation is observed without added hydrogen peroxide. On BSA, the major sites of modification were histidine and serine (Figure 3C).

The repeated phenomenon of  $H_2O_2$ -independent azidylation led to the hypothesis that lysozyme and BSA are noncovalently binding azide (BSA more tightly) in solution. We hypothesized that this binding is so tight that with BSA, at

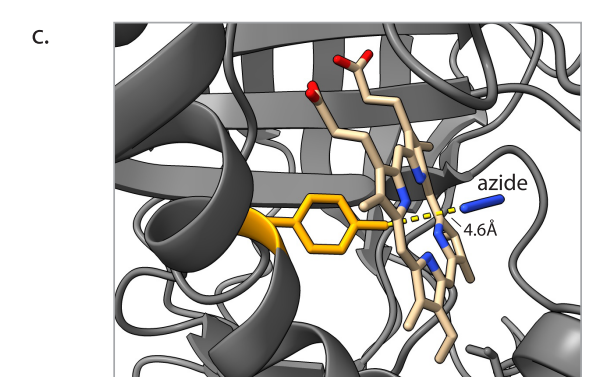
b.

d.

a.

Protein/Uniprot accession	Peptide identified	Azidylated residue(s)	PSMs
	VPTPTNSYTGIR	Not localized	8
G . 1 . 2 . 1 . 2 . 1 . 1 . 1 . 1 . 1 . 1	IFAYGDTQR	Y407	13
Catalase 3 / A0A1P8AWT7	LGPNYLQLPVNAPK	Y419	17
	TNIQEYWR	Y228 IYCR Not localized	7
	ELGVPIVMHDYLTGGFTANTSLSHYCR	Not localized	5
	YGRPLLGCTIKPK	Not localized	2
	LTYYTPEYETK	Y24	12
RuBisCo Large Subunit / O03042	TFQGPPHGIQVER	P151/P152/H153	16
	DNGLLLHIHR	H292/H294	39
	LSGGDHIHAGTVVGK	H326/H328	76
	ESTLGFVDLLR	L348/L349	16
Superoxide dismutase [Cu/Zn] 3/ Q9FK60	AVVVHADPDDLGK	V123	11

H294 H328 3.5Å



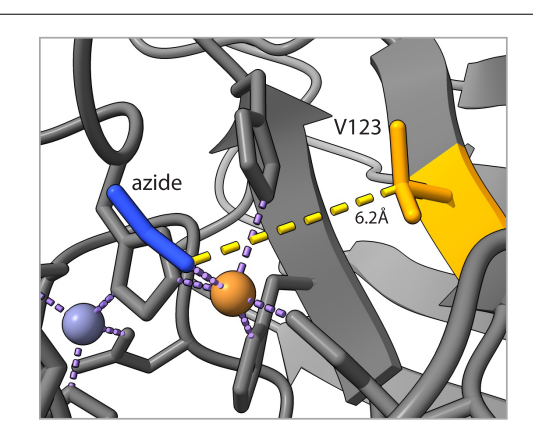


Figure 4. Azidylation in the soluble Arabidopsis proteome mainly occurs on rubisco and azide-binding proteins. (a) The majority of azidylation in Arabidopsis lysate occurs on rubisco, catalase, and superoxide dismutase. (b) On rubisco, the two strongest sites of azidylation (shown in orange) are buried within the active site, and in direct contact with transition state analogue 2-carboxyarabinitol-1,5,-bisphosphate (shown in blue) in the crystal structure (PDB: SIU0). (c) On catalase, the strongest site of azidylation is Y407 (shown in orange), which is conserved in *Bos taurus* catalase (shown here with azide co-crystallized), coordinates the heme group, and is <5 Å from azide bound in the crystal structure (PDB: 1TH2). The heme-bound iron has been hidden for better viewing. (d) The site of azidylation identified on Cu/Zn superoxide dismutase, V123, is conserved in *Saccharomyces cerevisiae* (shown here with azide co-crystallized) and is ~6 Å from the azide bound in the crystal structure (PDB: 1YAZ).

a minimum of 1 mM azide, some azide remains bound following stringent precipitation and buffer exchange methods. We thus asked whether small amounts of added azide are sufficient for concurrent BSA azidylation and clicking in the CuAAC reaction. If so, this would be consistent with BSA binding and carrying azide through precipitation at sufficient levels to observe the azidylation seen in the absence of added  $H_2O_2$ . This was indeed the case; as low as  $100~\mu M$  azide (a 10:1 azide/BSA molar ratio) added to a click reaction containing BSA that had never seen azide caused detectable azidylation above background (Figure S12 and Table S4). MS analysis confirmed that the modification is the identical +96.04 amu mass shift observed following photocleavage of  $H_2O_2$ -mediated azidylation as well, suggesting that this azidylation results in an identical adduct.

The distinct reaction conditions explored above presented unique situations for considering possible azidylation mechanisms. First, in the metal-free,  $H_2O_2$ -supplied reaction, we posit that the mechanism may be at least partially described by currently understood azido radical chemistry. Following azido radical generation by  $H_2O_2$ , the radical abstracts hydrogen from an available sidechain, after which a carbon radical intermediate either attacks an azide anion or recombines with a second azido radical, resulting in covalent azidylation. It is also possible that, as previously described, the azide radical directly adds to a carbon, especially in those cases of activated carbons within aromatic ring sidechains.  $^{17,18,21}$ 

Consistent with both mechanisms, subsequent clicking and cleaving forms the observed mass adduct. Canonically, azido radicals attack benzylic, aldehyde, and allylic bonds, a pattern that is not wholly observed here. Thus, it may be that some of the modifications we observe follow one of the possible mechanisms, whereas some do not. Future mechanistic studies will elaborate more upon the possible mechanism(s).

Second, in the click reaction, with both Cu(II) and ascorbate supplied, azidylation could be occurring differently. This reaction contains sufficient levels of Cu to catalyze metal-mediated azide transfer,  $^{14,32}$  so this could be a possible reaction mechanism. These reactions rely upon an oxidant—given that ascorbate and Cu may generate both hydroxyl radicals and  $H_2O_2$  as byproducts of their redox chemistry,  $^{33}$  we posit that the levels generated here in the click reaction are sufficient to enable metal-catalyzed azide transfer. If  $H_2O_2$  is generated in sufficient amounts, azidylation may occur to some degree as described above.

Finally, in the denaturing reaction containing 4 M urea, we observed modification in regions and on residues not seen previously, when azidylation is performed under physiological conditions (phosphate-buffered saline [PBS], pH 6–7). For example, as with lysozyme, a modified lysine was also observed on BSA, as well as a peptide containing either a modified leucine or valine (Figure S12 and Table S4). We take this increased azidylation to be a result of urea-based alterations in the 3D structure and dynamic intramolecular motion of the

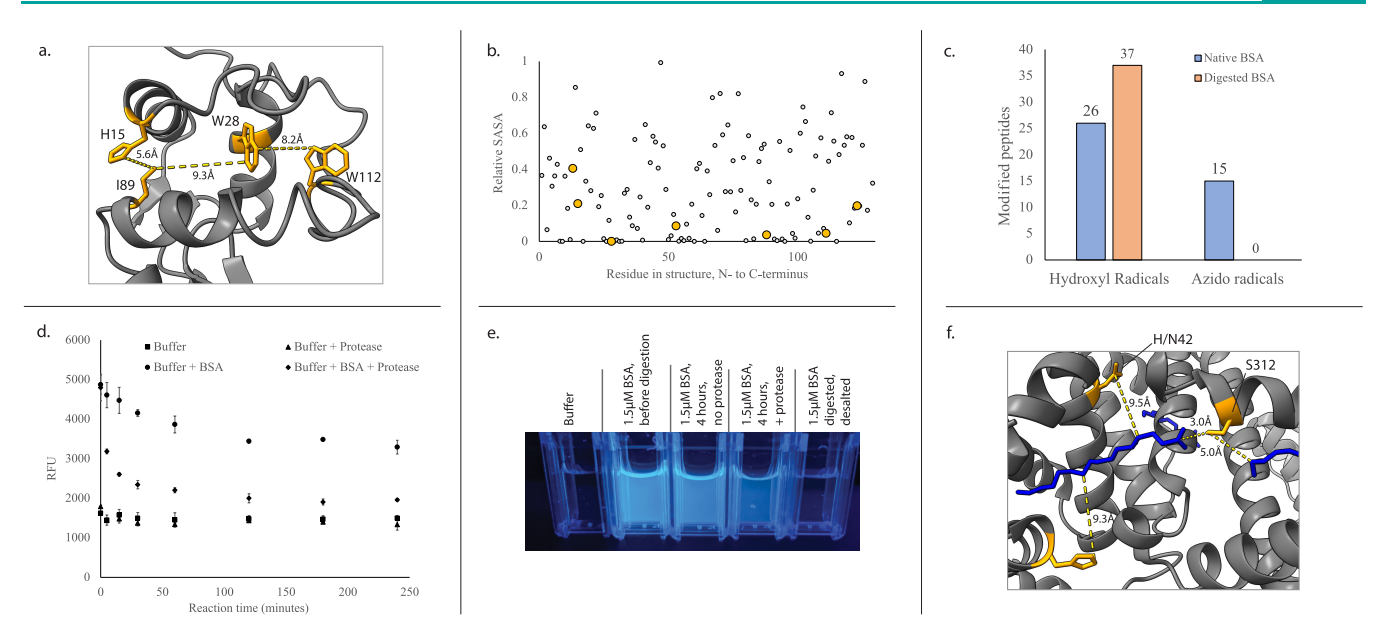


Figure 5. Azidylation occurs in solvent-inaccessible regions, requires higher-order protein structure, and labels residues in proximity to hydrophobic ligand-binding pockets. (a) Azidylated residues (orange) in lysozyme line a contiguous, buried cleft, and are aligned with one another (PDB: 8LYZ). (b) Lysozyme azidylation occurs mainly in solvent-inaccessible regions. Relative solvent-accessible surface area (SASA) is shown from N- to C-terminus, and orange dots are localized azidylated residues or short stretches. (c) Although digesting BSA to tryptic peptides prior to hydroxyl radical footprinting increases modification, as expected, given its correlation to solvent accessibility, digesting BSA prior to azidylation abolishes detectable modification entirely. (d) Digesting BSA reduces ANS binding and fluorescence in a time-dependent fashion. Data points are averages, and error bars are standard deviation from n = 3 fluorescent measurements of single samples. (e) Digesting BSA abolishes ANS binding and fluorescence, visualized with UV excitation. (f) Azidylated residues in BSA (orange) are near two bound palmitate molecules (blue), HSA cocrystallized with palmitate (PDB: 1E7H).

protein in solution and hypothesize that this "one-pot clicking" phenomenon is due to the oxidative nature of the CuAAC reaction combined with BSA's ability to bind azide. Furthermore, since denaturing conditions yield the observed increased azidylation, we would posit that the azidylation is conformationally sensitive and can putatively be used to detect or label discrete protein conformers (though as seen here in 4 M urea, they may not be native), which will be investigated further in future work. Altogether, the data obtained to date suggest that BSA is binding azide noncovalently, thereby supplying it to the click reaction and enabling the observed "one-pot" clicking.

2.4. Oxidative Azidylation in a Cell-Free Lysate of Arabidopsis thaliana Identifies Known Azide-Binding **Sites.** Given the above observations, we hypothesized that performing oxidative azidylation on a complex mixture would yield covalent modification on known azide-binding proteins. To test this, we azidylated an A. thaliana soluble proteome containing metabolites and buffer components, i.e., conditions different from the two pure model proteins which were simply dissolved in PBS. In contrast to the two pure proteins, we found that 400 mM azide, an acid-cleavable biotin alkyne (Figure 1C), and acquiring tandem mass spectra with HCD fragmentation provided the best survey of azidylated proteins, which we hypothesize is due to the dynamic range of a complex mixture vs a pure protein, the more complex buffering system, and increase in instrument duty cycle using HCD vs EThcD fragmentation. From this analysis, we identified 55 peptides containing the +125.06 amu mass adduct corresponding to azidylation from a range of proteins (Table S5). Low levels of azidylation were identified on a handful of proteins, for which no obvious commonality in terms of gene ontology or sequence motif enrichment was present. These included the

azide-binding protein cytochrome C, the  $\rm H_2O_2$ -removal enzymes peroxidase 38 and L-ascorbate peroxidase, a few transporters, and an array of other metabolic synthesis proteins.

The highest levels of azidylation identified from an Arabidopsis lysate occurred on rubisco, catalase, and Zn/Cu superoxide dismutase (Figure 4A). Notably, though this assay identified multiple known azide-binding proteins, the most azidylated protein was rubisco, which is likely due to its relatively massive abundance in plant tissue. The two major regions of azidylation identified on rubisco, H326/H328 and H292/H294, are adjacent to the catalytic site, and H294 and H328 are both within 6 Å of the bound transition state analogue 2-carboxyarabinitol-1,5-diphosphate in a recent crystal structure (Figure 4B).34 These four histidines are conserved between Arabidopsis and Galdieria rubisco, and are also within ~10 Å of both CO<sub>2</sub> and O<sub>2</sub> co-crystallized in the respective crystal structures (Figure S13).35 Multiple modified residues and regions, including the above, are spatially close (~15 Å apart at most) and suggest that azide may cluster within and near the catalytic site.

Catalase is well known to be inhibited by azide binding<sup>36,37</sup> noncovalently to the protein. Our experiments corroborated this and demonstrated that the cytosol was still catalytically active—when H<sub>2</sub>O<sub>2</sub> was added to our samples, native catalase quickly broke it down, resulting in significant foaming presumably due to the release of gaseous oxygen (not shown). The addition of azide prior to H<sub>2</sub>O<sub>2</sub> prevented this entirely, consistent with azide inhibiting this reaction. Thus, it was not surprising to observe four sites of covalent azidylation on catalase, as it can noncovalently bind azide. Three of the four sites were localized to Y228, Y407, and Y419. Of these, both Y407 and Y419 are conserved in *Bos taurus* catalase, for

which a crystal structure with bound azide has been solved. Examining the structure revealed that Y407, one of the major sites of azidylation identified here, directly coordinates the heme cofactor that interacts with bound azide (and  $H_2O_2$ , during catalysis), and azide is less than 5 Å from Y407 (Figure 4C). The second conserved site, Y419, is ~11 Å behind Y407. On Cu/Zn superoxide dismutase, only V123 was azidylated. This valine is conserved across multiple genera, <sup>39</sup> and mapping it on a crystal structure of *S. cerevisiae* Cu/Zn superoxide dismutase with bound azide revealed that it is directly proximal to the site of Cu coordination, pointed into the catalytic site, and ~6 Å from the bound, co-crystallized azide (Figure 4D). <sup>40</sup>

In the case of rubisco, which is not known to require or coordinate metal cofactors, azidylation is likely occurring via hydrogen abstraction and anion attack or radical recombination as described above, whereas it may be that for catalase and superoxide dismutase, the metal or metal-containing heme cofactor not only coordinates azide but also facilitates covalent addition, consistent with previously described reaction mechanisms. 14,32 So as with pure proteins in solution, azidylation in a complex protein mixture may also proceed via multiple mechanisms. That said, the most abundant azidylation events on known azide-binding proteins were clearly identified with angstrom-level precision using azide cocrystal structures as references (Figure 4C,D), suggesting that the method can be used to capture and map noncovalent azide binding. Overall, azidylating a cell-free tissue lysate composed of the soluble Arabidopsis proteome demonstrated that azidylation occurring in a complex protein background and buffer system corroborated previously observed noncovalent azide binding and identified putative novel azide-binding pockets using the azido radical as an "affinity" reagent.

2.5. Azide Binds Hydrophobic Patches on Structured **Proteins.** We next considered what principle(s) could drive the protein/azide binding that oxidative azidylation maps. In protein footprinting experiments, solvent-accessible surface area (SASA) is a major factor that drives labeling, but we found that this was not the case for azidylation. On lysozyme, of the seven azidylated residues, H15, W28, I88, and W111 are within a contiguous, totally buried cleft sandwiched by three alpha helices and with their sidechains pointed inward, aligned, and solvent-inaccessible (Figure 5A). Additionally, calculating solvent accessibility from the crystal structure demonstrated that these four residues are among the least solvent-accessible in the whole protein, and the total group of modified residues exhibits no correlation with SASA (Figure 5B), 41 a result we also saw with BSA, rubisco, catalase, and Cu/Zn superoxide dismutase (Figures S14-S17). This result was striking and recalled similar behavior previously reported with the covalent protein label DEPC, which labels hydrophobic patches on intact, structured proteins.<sup>27</sup> These observations with azide and DEPC stand in sharp contrast to other covalent footprinting reagents, such as hydroxyl radicals, which, because they probe SASA, exhibit increased modification following denaturation of a protein's 3D structure.

To further the comparison of azidylation with DEPC, we investigated azidylating tryptic BSA peptides vs intact protein. Previously, although protein pre-digested into peptides prior to hydroxyl radical footprinting demonstrates significantly more labeling than native protein, <sup>42</sup> DEPC labeling is strongly reduced on tryptic peptides relative to intact protein. <sup>27</sup> This suggests that higher-order structure, rather than SASA, is necessary for DEPC labeling. We performed an analogous

experiment with BSA and azide and found that no azidylation was detected on digested peptide samples across multiple replicates and concurrently azidylated native BSA expected levels (Figures 5C, S18, and S19, Table S6). Thus, like DEPC, a higher-order structure is required for radical-mediated protein azidylation, and digesting BSA to tryptic peptides prior to azidylation reduces modification to below the limit of detection, if not entirely. We next labeled BSA with DEPC to assay overlap in regions of DEPC modification and azidylation. At a molar ratio of 1:1 DEPC/BSA, 6 out of 9 sites that were azidylated with 100 mM azide, and 4 out of 5 sites that were azidylated with 10 mM azide, were within peptides labeled with DEPC across multiple replicates with C.V. values < 30% (Figure S20 and Table S7). We consider this reasonable agreement considering the differing chemical mechanisms (radical vs nucleophilic attack), the difference in size of the two reagents, and the difference in residue reactivities between the two reagents. Based on these results, we reasoned that, like DEPC, azide may also be probing hydrophobic patches created by higher-order protein structures.

To investigate this further, we asked whether another established probe of protein structure and hydrophobicity, the fluorescent molecule 8-anilinonaphthalene-1-sulfonic acid (ANS),<sup>43,44</sup> exhibits similar behavior to azide. This was the case. As full-length BSA is digested to peptides with proteases, we found that ANS fluorescence significantly decreases over time, and that completely digested, BSA-derived peptides, even when supplied in much higher concentrations than intact BSA, cause no detectable ANS fluorescence (Figures 5D,E and S21).

Serum albumins have a significant role in lipid biology—in blood, they bind fatty acids of many types with high affinity via noncovalent hydrophobic interaction. <sup>45–47</sup> A structure for BSA co-crystallized with palmitate does not exist; however, human serum albumin (HSA), which exhibits significant sequence and structural similarity to BSA, has been crystallized with bound palmitate. <sup>46,47</sup> Aligning the sequences and mapping BSA azidylation to the HSA/palmitate structure revealed that three of the five sites that are azidylated with 10 mM azide, which we take to be higher-affinity binding sites, are within 11 Å of a pocket in HSA that binds two palmitate molecules, and the only residue azidylated with 1 mM azide, S310, conserved in HSA as S312, is within 5.0 Å of each palmitate (Figure 5F).

Taken together, the cumulative data support a model in which direct and covalent protein azidylation occurs on threedimensional, hydrophobic regions that may be buried and only present in folded proteins. Crystal structures of azide bound to known targets, such as F1-ATPase, indicate, via proximity to charged groups in the ligand binding sites, that ionic interactions are involved.<sup>23</sup> These occur between the partially positive internal N atom and negatively charged terminal phosphate of adenosine diphosphate, as well as interactions of the anionic terminal N atoms of azide with cationic partners, such as the amino group of lysine residues. Based on the work reported herein, we suggest that hydrophobic properties of the azide molecule may also be considered in fully understanding the noncovalent binding of azide to target proteins in cells. Furthermore, given the covalent azidylation we observe in the active sites of proteins like rubisco, that were not previously considered to be azide targets, a closer examination of azide interactions with a larger number of proteins in general should be considered. These studies could consider our model invoking potential hydrophobic interactions of azide pi electrons with either cations or with pi electrons in aromatic

amino acid sidechains in addition to purely ionic interactions to explain the biochemical role of the azide. Though the complex protein mixture we azidylated here was clarified of membranes, we also propose that the azide radical might also label transmembrane domains in hydrophobic polytopic proteins, which DEPC has been shown to do,<sup>24</sup> and will be the subject of future experiments.

#### 3. CONCLUSIONS

Recent advances have been made that greatly expand the utility of covalent labeling reagents for mapping interacting surfaces and for reporting on conformational changes in soluble proteins. <sup>30,48–50</sup> For example, new reagents have been developed that can react with aromatic sidechains within membrane proteins and on hydrophobic patches, 24-27 and a handful of recently developed methods are aimed at measuring proteome-wide conformational changes.<sup>48-54</sup> In this report, while we set out to exploit the azido radical as a simpler means of general covalent protein labeling and subsequent derivatization, the product of these experiments is also a method for covalently modifying protein with the azido radical that captures and identifies locations of noncovalent azide binding. With our method, azide may present a unique, enrichable method to add to the existing toolbox. The data point to a model in which the small size of the azide anion/free radical may allow its diffusion into hydrophobic cavities that are inaccessible to larger reagents. As with other modifications (e.g., phosphorylation), an enrichment method is currently essential for MS analysis of azidylation.<sup>55</sup> That said, the ability to capture and enrich for azidylated peptides described here enables facile observation of low stoichiometric events and azidylation from a complex mixture. Future efforts will also further examine the azide radical's ability to label discrete protein conformations, both with model proteins and, given the enrichable nature of azidylation, with complex mixtures of proteins in lysates, to examine proteome-wide conformational changes. In conclusion, we report a working model in which three-dimensional protein hydrophobic microenvironments of soluble proteins can be identified by oxidatively radicalizing the azide anion to directly azidylate amino acid sidechains, which can then be captured and identified using mass spectrometry. Beyond empirically mapping hydrophobicity, azide radicalmediated azidylation also presents a simple and fast means for click-based derivatization of proteins in vitro using known reagents available in any lab, as a new way to enable chemical biology and synthetic protein chemistry.

#### ASSOCIATED CONTENT

#### Supporting Information

The Supporting Information is available free of charge at https://pubs.acs.org/doi/10.1021/acschembio.3c00224.

Additional experimental methods, materials, and details; example mass spectra; GFP and ANS fluorescence data; oxidation data; further crystal structures; solvent accessibility charts; and DEPC labeling data (Figures S1–S21) (PDF)

Raw output from Proteome Discoverer searches of raw MS data (XLSX)

15N\_BSA\_Azidylation (XLSX)

BSA\_DoseCurve (XLSX)

BSA OnePot (XLSX)

ArabdopsisLysate MSOutput (XLSX)

Native\_Digest\_Data (XLSX)
DEPC\_labeling (XLSX)

#### AUTHOR INFORMATION

#### **Corresponding Author**

Michael R. Sussman — Center for Genomic Science Innovation, University of Wisconsin—Madison, Madison, Wisconsin 53706, United States; Department of Biochemistry, University of Wisconsin—Madison, Madison, Wisconsin 53706, United States; Email: msussman@wisc.edu

#### **Authors**

Benjamin B. Minkoff — Center for Genomic Science Innovation, University of Wisconsin—Madison, Madison, Wisconsin S3706, United States; orcid.org/0000-0001-9807-0354

**Heather L. Burch** – Center for Genomic Science Innovation, University of Wisconsin—Madison, Madison, Wisconsin 53706, United States

Jamison D. Wolfer – Center for Genomic Science Innovation, University of Wisconsin—Madison, Madison, Wisconsin 53706, United States

Complete contact information is available at: https://pubs.acs.org/10.1021/acschembio.3c00224

#### **Author Contributions**

All authors conceived of experiments and interpreted results. H.L.B. and B.B.M. performed experiments. B.B.M. and M.R.S. wrote the manuscript. All authors edited the manuscript.

#### **Funding**

This research was funded by awards HDTRA1-16-1-0049 from the Department of Defense, Defense Threat Reduction Agency to M.R.S., 2010789-IOS-PGRP and 1943816-MCB from the National Science Foundation to M.R.S., and DE-FG02-8ER13938 from the Department of Energy to M.R.S.

#### Notes

The authors declare the following competing financial interest(s): All authors are inventors on a provisional patent application, assigned to Wisconsin Alumni Research Foundation, surrounding the described technique.

#### ACKNOWLEDGMENTS

The authors gratefully acknowledge G. Phillips and I. Rayment for discussion during preparation of the manuscript, and S. Gellman and the reviewers for their comments during the review process.

#### ABBREVIATIONS

BSA, bovine serum albumin; OH, hydroxyl; HRF, hydroxyl radical footprinting; DEPC, diethylpyrocarbonate; CuAAC, copper-catalyzed azide—alkyne cyclocaddition; MS, mass spectrometry; SDS-PAGE, sodium dodecyl sulfate—polyacrylamide gel electrophoresis; HCD, high-energy collisional dissociation; EThcD, electron transfer dissociation with supplemental high-energy collisional dissociation; SASA, solvent-accessible surface area; ANS, 8-anilinonaphthalene-1-sulfonic acid; HSA, human serum albumin

#### REFERENCES

(1) Lins, L.; Brasseur, R. The hydrophobic effect in protein folding. FASEB J. 1995, 9, 535–540.

- (2) Sarkar, A.; Kellogg, G. E. Hydrophobicity-shake flasks, protein folding and drug discovery. *Curr. Top. Med. Chem.* **2010**, *10*, 67–83.
- (3) McKenzie-Coe, A.; Montes, N. S.; Jones, L. M. Hydroxyl radical protein footprinting: A mass spectrometry-based structural method for studying the higher order structure of proteins. *Chem. Rev.* **2022**, 122, 7532–7561.
- (4) Liu, X. R.; Zhang, M. M.; Gross, M. L. Mass spectrometry-based protein footprinting for higher-order structure analysis: Fundamentals and applications. *Chem. Rev.* **2020**, *120*, 4355–4454. From NLM Medline.
- (5) Huang, W.; Ravikumar, K. M.; Chance, M. R.; Yang, S. Quantitative mapping of protein structure by hydroxyl radical footprinting-mediated structural mass spectrometry: a protection factor analysis. *Biophys. J.* **2015**, *108*, 107–115.
- (6) Patterson, D. M.; Nazarova, L. A.; Prescher, J. A. Finding the right (bioorthogonal) chemistry. ACS Chem. Biol. 2014, 9, 592-605.
- (7) Scinto, S. L.; Bilodeau, D. A.; Hincapie, R.; Lee, W.; Nguyen, S. S.; Xu, M.; Am Ende, C. W.; Finn, M. G.; Lang, K.; Lin, Q.; et al. Bioorthogonal chemistry. *Nat. Rev. Methods Primers* **2021**, *1*, 30.
- (8) Inoue, N.; Onoda, A.; Hayashi, T. Site-specific modification of proteins through N-terminal azide labeling and a chelation-assisted CuAAC reaction. *Bioconjugate Chem.* **2019**, *30*, 2427–2434.
- (9) van Dongen, S. F.; Teeuwen, R. L.; Nallani, M.; van Berkel, S. S.; Cornelissen, J. J.; Nolte, R. J.; van Hest, J. C. Single-step azide introduction in proteins via an aqueous diazo transfer. *Bioconjugate Chem.* **2009**, 20, 20–23.
- (10) Schoffelen, S.; van Eldijk, M. B.; Rooijakkers, B.; Raijmakers, R.; Heck, A. J.; van Hest, J. C. Metal-free and pH-controlled introduction of azides in proteins. *Chem. Sci.* **2011**, *2*, 701–705.
- (11) Shee, M.; Singh, N. D. P. Chemical versatility of azide radical: journey from a transient species to synthetic accessibility in organic transformations. *Chem. Soc. Rev.* **2022**, *51*, 2255–2312.
- (12) Jiang, X.; Hao, X.; Jing, L.; Wu, G.; Kang, D.; Liu, X.; Zhan, P. Recent applications of click chemistry in drug discovery. *Expert Opin. Drug Discovery* **2019**, *14*, 779–789.
- (13) Sivaguru, P.; Ning, Y.; Bi, X. New strategies for the synthesis of aliphatic azides. *Chem. Rev.* **2021**, *121*, 4253–4307.
- (14) Huang, X.; Groves, J. T. Taming azide radicals for catalytic C—H azidation. *ACS Catal.* **2016**, *6*, 751–759.
- (15) Minisci, F.; Galli, R. Influence of the electrophilic character on the reactivity of free radicals in solution reactivity of alkoxy, hydroxy, alkyl and azido radicals in presence of olefins. *Tetrahedron Lett.* **1962**, 3, 533–538.
- (16) Minisci, F.; Galli, R. Reactivity of hydroxy and alkoxy radicals in presence of olefins and oxidation-reduction systems. Introduction of azido, chloro and acyloxy groups in allylic position and azido-chlorination of olefins. *Tetrahedron Lett.* **1963**, *4*, 357–360.
- (17) Singh, A.; Koroll, G. W.; Cundall, R. B. Pulse radiolysis of aqueous solutions of sodium azide: reactions of azide radical with tryptophan and tyrosine. *Radiat. Phys. Chem.* (1977) **1982**, 19, 137–146.
- (18) Butler, J.; Land, E. J.; Swallow, A. J.; Prutz, W. The azide radical and its reaction with tryptophan and tyrosine. *Radiat. Phys. Chem.* (1977) **1984**, 23, 265–270.
- (19) Lambert, C.; Edward, J.; et al. Role of azide concentration in pulse radiolysis studies of oxidation: 3, 4-dihydroxyphenylalanine. *J. Chem. Soc., Faraday Trans.* **1991**, 87, 2939–2942.
- (20) Gatin, A.; Billault, I.; Duchambon, P.; Van der Rest, G.; Sicard-Roselli, C. Oxidative radicals (HO• or N3•) induce several di-tyrosine bridge isomers at the protein scale. *Free Radical Biol. Med.* **2021**, *162*, 461–470
- (21) Land, E. J.; Prutz, W. A. Reaction of azide radicals with amino acids and proteins. *Int. J. Radiat. Biol. Relat. Stud. Phys., Chem. Med.* 1979, 36, 75–83.
- (22) Kolb, H. C.; Finn, M. G.; Sharpless, K. B. Click chemistry: Diverse chemical function from a few good reactions. *Angew. Chem., Int. Ed.* **2001**, *40*, 2004–2021.

- (23) Bowler, M. W.; Montgomery, M. G.; Leslie, A. G.; Walker, J. E. How azide inhibits ATP hydrolysis by the F-ATPases. *Proc. Natl. Acad. Sci. U.S.A.* **2006**, *103*, 8646–8649.
- (24) Guo, C.; Cheng, M.; Li, W.; Gross, M. L. Diethylpyrocarbonate footprints a membrane protein in micelles. *J. Am. Soc. Mass Spectrom.* **2021**, 32, 2636–2643.
- (25) Sun, J.; Liu, X. R.; Li, S.; He, P.; Li, W.; Gross, M. L. Nanoparticles and photochemistry for native-like transmembrane protein footprinting. *Nat. Commun.* **2021**, *12*, No. 7270. From NLM Medline.
- (26) Sun, J.; Li, W.; Gross, M. L. Advances in mass spectrometry-based footprinting of membrane proteins. *Proteomics* **2022**, 22, No. 2100222. From NLM Medline.
- (27) Limpikirati, P.; Pan, X.; Vachet, R. W. Covalent labeling with diethylpyrocarbonate: Sensitive to the residue Microenvironment, providing improved analysis of protein higher order structure by mass spectrometry. *Anal. Chem.* **2019**, *91*, 8516–8523. From NLM Medline.
- (28) Rego, N. B.; Xi, E.; Patel, A. J. Identifying hydrophobic protein patches to inform protein interaction interfaces. *Proc. Natl. Acad. Sci. U.S.A.* **2021**, *118*, No. e2018234118.
- (29) West, G. M.; Tang, L.; Fitzgerald, M. C. Thermodynamic analysis of protein stability and ligand binding using a chemical modification-and mass spectrometry-based strategy. *Anal. Chem.* **2008**, *80*, 4175–4185.
- (30) Wiebelhaus, N.; Singh, N.; Zhang, P.; Craig, S. L.; Beratan, D. N.; Fitzgerald, M. C. Discovery of the xenon—protein interactome using large-scale measurements of protein folding and stability. *J. Am. Chem. Soc.* **2022**, *144*, 3925—3938.
- (31) Martell, J.; Weerapana, E. Applications of copper-catalyzed click chemistry in activity-based protein profiling. *Molecules* **2014**, *19*, 1378–1393. From NLM Medline.
- (32) Goswami, M.; de Bruin, B. Metal-catalysed azidation of organic molecules. *Eur. J. Org. Chem.* **2017**, 2017, 1152–1176. From NLM PubMed-not-MEDLINE.
- (33) Shen, J.; Griffiths, P. T.; Campbell, S. J.; Utinger, B.; Kalberer, M.; Paulson, S. E. Ascorbate oxidation by iron, copper and reactive oxygen species: review, model development, and derivation of key rate constants. *Sci. Rep.* **2021**, *11*, No. 7417. From NLM PubMed-not-MEDLINE.
- (34) Valegård, K.; Hasse, D.; Andersson, I.; Gunn, L. H. Structure of Rubisco from *Arabidopsis thaliana* in complex with 2-carboxyarabinitol-1,5-bisphosphate. *Acta Crystallogr., Sect. D: Struct. Biol.* **2018**, 74, 1–9. From NLM Medline.
- (35) Stec, B. Structural mechanism of RuBisCO activation by carbamylation of the active site lysine. *Proc. Natl. Acad. Sci. U.S.A.* **2012**, *109*, 18785–18790. From NLM Medline.
- (36) Nicholls, P. The reaction of azide with catalase and their significance. *Biochem. J.* **1964**, *90*, 331–343. From NLM Medline.
- (37) Thurman, R. G.; Chance, B. Inhibition of catalase in perfused rat liver by sodium azide. *Ann. N. Y. Acad. Sci.* **1969**, *168*, 348–353. From NLM Medline.
- (38) Sugadev, R.; Ponnuswamy, M. N.; Sekar, K. Structural analysis of NADPH depleted bovine liver catalase and its inhibitor complexes. *Int. J. Biochem. Mol. Biol.* **2011**, *2*, *67*. From NLM PubMed-not-MEDLINE.
- (39) Perry, J. J.; Shin, D. S.; Getzoff, E. D.; Tainer, J. A. The structural biochemistry of the superoxide dismutases. *Biochim. Biophys. Acta, Proteins Proteomics* **2010**, *1804*, 245–262. From NLM Medline.
- (40) Hart, P. J.; Balbirnie, M. M.; Ogihara, N. L.; Nersissian, A. M.; Weiss, M. S.; Valentine, J. S.; Eisenberg, D. A structure-based mechanism for copper-zinc superoxide dismutase. *Biochemistry* **1999**, 38, 2167–2178. From NLM Medline.
- (41) Beddell, C. R.; Blake, C. C.; Oatley, S. J. An x-ray study of the structure and binding properties of iodine-inactivated lysozyme. *J. Mol. Biol.* **1975**, *97*, 643–654. From NLM Medline.
- (42) Minkoff, B. B.; Blatz, J. M.; Choudhury, F. A.; Benjamin, D.; Shohet, J. L.; Sussman, M. R. Plasma-generated OH radical

production for analyzing three-dimensional structure in protein therapeutics. *Sci. Rep.* **2017**, *7*, No. 12946.

- (43) Ota, C.; Tanaka, S. I.; Takano, K. Revisiting the rate-limiting step of the ANS-protein binding at the protein surface and inside the hydrophobic cavity. *Molecules* **2021**, *26*, 420–432. From NLM Medline.
- (44) Togashi, D. M.; Ryder, A. G. A fluorescence analysis of ANS bound to bovine serum albumin: binding properties revisited by using energy transfer. *J. Fluoresc.* **2008**, *18*, 519–526.
- (45) Reed, R. G. Location of long chain fatty acid-binding sites of bovine serum albumin by affinity labeling. *J. Biol. Chem.* **1986**, *261*, 15619–15624.
- (46) Bujacz, A. Structures of bovine, equine and leporine serum albumin. *Acta Crystallogr., Sect. D: Biol. Crystallogr.* **2012**, *68*, 1278–1289
- (47) Bhattacharya, A. A.; Grune, T.; Curry, S. Crystallographic analysis reveals common modes of binding of medium and long-chain fatty acids to human serum albumin. *J. Mol. Biol.* **2000**, *303*, 721–732.
- (48) Ma, R.; Meng, H.; Wiebelhaus, N.; Fitzgerald, M. C. Chemoselection strategy for limited proteolysis experiments on the proteomic scale. *Anal. Chem.* **2018**, *90*, 14039–14047. From NLM Medline.
- (49) Espino, J. A.; King, C. D.; Jones, L. M.; Robinson, R. A. S. In vivo fast photochemical oxidation of proteins using enhanced multiplexing proteomics. *Anal. Chem.* **2020**, *92*, 7596–7603. From NLM Medline.
- (50) Jiao, F.; Yu, C.; Wheat, A.; Wang, X.; Rychnovsky, S. D.; Huang, L. Two-dimensional fractionation method for proteome-wide cross-linking mass spectrometry analysis. *Anal. Chem.* **2022**, *94*, 4236–4242. From NLM Medline.
- (51) Jones, L. M. Mass spectrometry-based methods for structural biology on a proteome-wide scale. *Biochem. Soc. Trans.* **2020**, 48, 945–954. From NLM Medline.
- (52) Cappelletti, V.; Hauser, T.; Piazza, I.; Pepelnjak, M.; Malinovska, L.; Fuhrer, T.; Li, Y.; Dorig, C.; Boersema, P.; Gillet, L.; et al. Dynamic 3D proteomes reveal protein functional alterations at high resolution in situ. *Cell* **2021**, *184*, 545–559 e522. From NLM Medline.
- (53) Mateus, A.; Kurzawa, N.; Perrin, J.; Bergamini, G.; Savitski, M. M. Drug target identification in tissues by thermal proteome Profiling. *Annu. Rev. Pharmacol. Toxicol.* **2022**, *62*, 465–482. From NLM Medline.
- (54) Wiebelhaus, N.; Singh, N.; Zhang, P.; Craig, S. L.; Beratan, D. N.; Fitzgerald, M. C. Discovery of the xenon-protein interactome using large-scale measurements of protein folding and stability. *J. Am. Chem. Soc.* **2022**, *144*, 3925–3938. From NLM Medline.
- (55) Huang, J.; Wang, F.; Ye, M.; Zou, H. Enrichment and separation techniques for large-scale proteomics analysis of the protein post-translational modifications. *J. Chromatogr. A* **2014**, *1372*, 1–17. From NLM PubMed-not-MEDLINE.

### **□** Recommended by ACS

## Folding-Assisted Peptide Disulfide Formation and Dimerization

Clara G. Victorio and Nicholas Sawyer

JUNE 30, 2023

ACS CHEMICAL BIOLOGY

READ 🗹

#### Biocompatible Lysine Protecting Groups for the Chemoenzymatic Synthesis of K48/K63 Heterotypic and Branched Ubiquitin Chains

Toshiki Mikami, Jeffrey W. Bode, et al.

JULY 15, 2023

ACS CENTRAL SCIENCE

READ 🗹

## Comparison of Integrin $\alpha IIb\beta 3$ Transmembrane Association in Vesicles and Bicelles

Alan J. Situ and Tobias S. Ulmer

JUNE 06, 2023 BIOCHEMISTRY

READ 🗹

#### Pyroglutamination-Induced Changes in the Physicochemical Features of a CXCR4 Chemokine Peptide: Kinetic and Structural Analysis

Mariana M. L. Ferreira, Clovis R. Nakaie, et al.

AUGUST 04, 2023

BIOCHEMISTRY

READ 🗹

Get More Suggestions >